RKKY Interactions and the Anomalous Hall Effect in Metallic Rare-Earth Pyrochlores

SungBin Lee,[1] Arun Paramekanti,[1,2] and Yong Baek Kim[1,2,3]
[1]*Department of Physics, University of Toronto, Toronto, Ontario M5S 1A7, Canada*
[2]*Canadian Institute for Advanced Research, Toronto, Ontario M5G 1Z8, Canada*
[3]*School of Physics, Korea Institute for Advanced Study, Seoul 130-722, Korea*
(Received 21 May 2013; published 4 November 2013)

Motivated by experiments on $Pr_2Ir_2O_7$, we consider metallic pyrochlore systems $A_2B_2O_7$, where the A sites are occupied by rare-earth local moments and the B sites host $5d$ transition metal ions with itinerant strongly spin-orbit coupled electrons. Assuming non-Kramers doublets on the A site, we derive the RKKY interaction between them mediated by the B-site itinerant electrons and find extended non-Heisenberg interactions. Analyzing a simplified model of the RKKY interaction, we uncover a local moment phase with coexisting spiral Ising-like magnetic dipolar and XY-like quadrupolar ordering. This state breaks time-reversal and lattice symmetries, and reconstructs the B-site electronic band structure, producing a Weyl metallic phase with an intrinsic anomalous Hall effect and an undetectably small magnetization. We discuss implications of our results for $Pr_2Ir_2O_7$.

DOI: 10.1103/PhysRevLett.111.196601 PACS numbers: 72.15.Qm, 75.10.Lp, 75.70.Tj

The metallic pyrochlores, $A_2B_2O_7$, with a rare-earth A-site ion and a $5d$ transition metal B-site ion, lie at the intersection of exciting recent developments in physics. The A-site rare-earth moments on one pyrochlore sublattice could form quantum spin ice [1,2] from Ising anisotropy and geometric frustration, a feature they share with the insulating pyrochlores. The strongly spin-orbit coupled $5d$ conduction electrons, on the other hand, contain seeds of topological phases like Weyl semimetals or topological insulators [3–9]. The interplay of these two effects could pave the way for new emergent phenomena. The pyrochlore iridate $Pr_2Ir_{25}O_7$ provides an example of such a metallic frustrated system, with a significant Curie-Weiss (CW) temperature $\theta_{CW} \approx -20$ K [10–13]. For $T \lesssim 1.7$ K, even when an applied magnetic field along the $\langle 111 \rangle$ direction is removed, it exhibits a significant anomalous Hall effect (AHE) which grows upon cooling [14–16], although, in contrast to $Nd_2Mo_2O_7$, the uniform magnetization is undetectably small over a range of temperatures [17]. This raises the fundamental issue of mechanisms underlying the AHE [18] in materials with geometric frustration and strong spin-orbit coupling.

Motivated by the spin-ice physics observed in insulating pyrochlores $Pr_2Sn_2O_7$ or $Pr_2Zr_2O_7$, it has been proposed that the Ir electrons moving in the background of noncoplanar icelike Pr moments pick up Berry phases, leading to the observed AHE in the presence of a net spin chirality [16,19–21], analogous to that in manganites [22]. Such chiral order within the spin-ice manifold may be driven by a chiral RKKY interaction due to the Ir electrons [21]. However, the fact that θ_{CW} in $Pr_2Ir_2O_7$ is much larger than, and opposite in sign, to $Pr_2Sn_2O_7$ or $Pr_2Zr_2O_7$ suggests that the RKKY interaction may lead to significant deviations of the local moment physics from spin-ice behavior. Further, most previous studies, except Ref. [23], do not consider the microscopic nonlocal antiferromagnetic Kondo coupling between the Ir electrons and Pr moments. Motivated by this, we study, in this Letter, an alternative route to an AHE in metallic rare-earth pyrochlores, due to unusual ordering of the non-Kramers rare-earth moments driven by RKKY interactions.

When the f moment is a non-Kramers doublet, such as in Pr^{3+}, the pseudospin component τ^z along the local $\langle 111 \rangle$ direction carries a magnetic dipole moment and couples to the conduction electron spin density, while the $\tau^{x,y}$ components carry a quadrupole moment and couple to the electronic charge density. We show that the resulting RKKY coupling has a highly non-Heisenberg form and extends beyond the nearest neighbor term. We propose and study such a simplified spin model for non-Kramers doublets using a variational analysis. We find a rich phase diagram, shown in Fig. 1, which includes incommensurate spiral "coexistence" states (CE_1, CE_2), with wave vectors $(0, q, \pi)$ or $(0, 0, q)$, having spatially modulated, magnetic (dipolar) and quadrupolar order, i.e., "magnetoquadrupolar supersolids." We confirm that such a CE_2 state also exists within a classical Monte Carlo simulation. Although the CE_2 state has no net local moment magnetization, it reconstructs the band structure of the $5d$ electrons, producing Weyl points as well as small Fermi pockets, leading to a measurable AHE and an extremely small conduction electron magnetization [24]. We discuss possible implications for $Pr_2Ir_2O_7$.

Basic microscopic details and RKKY coupling.—The Pr^{3+} ion in $Pr_2Ir_2O_7$ is in a $4f^2$ configuration, with electron interactions and spin-orbit coupling favoring a total angular momentum state with $J = 4$. This ninefold degenerate manifold is split by crystal fields with D_{3d} point group symmetry around the Pr^{3+} ion. The splitting is captured by an effective time-reversal invariant crystal field

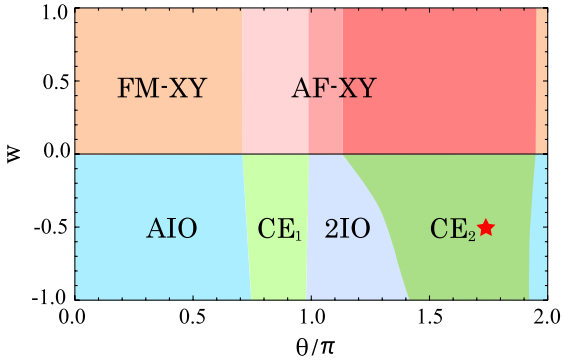

FIG. 1 (color online). Variational phase diagram of the pseudospin Hamiltonian in Eq. (2) relevant to RKKY coupled non-Kramers doublets, as a function of anisotropy w and $\theta = \tan^{-1}(J_2/J_1)$, obtained in the classical spin limit. For $w > 0$, we find ferromagnetic XY (FM-XY), antiferromagnetic XY (AF-XY), where spins order in the plane transverse to the local $\langle 111\rangle$ axes. These time-reversal invariant states display modulated quadrupolar order. For $w < 0$, we find Ising all-in-all-out (AIO) states, Ising two-in-two-out (2IO) states, and states with coexisting modulated Ising-XY orders (CE_1, CE_2).

Hamiltonian expressed in terms of $J = 4$ angular momentum operators, $H_{\rm cef} = -\alpha J_z^2 + \beta[J_z(J_+^3 + J_-^3) + \text{H.c.}] + \gamma(J_+^6 + J_-^6)$, with $\alpha > 0$, leading to a ground state non-Kramers doublet with a dominant $|J_z = \pm 4\rangle$ component, and a significant admixture of $|J_z = \pm 1\rangle$ and $|J_z = \mp 2\rangle$ [25]. Projection to this doublet allows us to define pseudospin-1/2 operators $\boldsymbol{\tau}$ with $\tau^z \propto J_z$ and $\tau^{\pm} \propto \{J_{\pm}, J_z\}$. Under time-reversal, $\tau^z \longrightarrow -\tau^z$, transforming as the magnetic dipole moment, while $\tau^{x,y}$ are left invariant, transforming like a quadrupole moment.

For Ir^{4+} electrons, strong spin-orbit coupling in the t_{2g} manifold leads to a half-filled effective $j = 1/2$ band. Since $Pr_2Ir_2O_7$ is metallic, we use an effective tight binding (tb) model for the Ir bands,

$$H_{\rm tb} = \sum_{ij}\sum_{\alpha\beta} c_{i\alpha}^{\dagger}(t_{ij}\delta_{\alpha\beta} + i\boldsymbol{v}_{ij}\cdot\boldsymbol{\sigma}_{\alpha\beta})c_{j\beta}, \qquad (1)$$

where $c_{i\alpha}^{\dagger}(c_{j\beta})$ denotes the electron creation (annihilation) operator at site i with the Kramers pseudospin index α corresponding to $j_z = \pm 1/2$, and $\boldsymbol{\sigma} = (\sigma^x, \sigma^y, \sigma^z)$ are Pauli matrices. We set $t_{ij} = t\,(t')$ for nearest (next-nearest) neighbors, and $\boldsymbol{v}_{ij} \neq 0$ for nearest-neighbors, with its direction fixed by lattice symmetries [26].

The coupling of the non-Kramers doublet to the B-site conduction electrons is unusual. Time-reversal invariance dictates that the Ising component of the A-site pseudospin τ_j^z at site j (which points along the local $\langle 111\rangle$ axis) couples to spin density $j_i^{\mu} = c_{i\alpha}^{\dagger}(\sigma_{\alpha\beta}^{\mu}/2)c_{i\beta}$ of electrons on the six neighboring B sites [23], while the planar components of the pseudospin $\tau_j^{\pm}$ couple to the charge density $n_i = c_{i\alpha}^{\dagger}c_{i\alpha}$ on the neighboring B sites. Keeping $j_i^{\mu}\tau_j^z$ and $n_i\tau_j^{\pm}$ terms, we find the symmetry allowed Kondo coupling H_{AB} with three parameters c_1, c_2, c_3. We then integrate out the conduction electrons to obtain the RKKY coupling between local moments (see the Supplemental Material [27]). The resulting RKKY interaction has two important features which are insensitive to the details of the Ir band structure: (i) it allows for significant couplings beyond the nearest-neighbor interaction, but is entirely negligible beyond the third neighbor; (ii) it is highly anisotropic in spin-space since $\tau^{x,y}$ and τ^z interact very differently with the spin-orbit coupled conduction band.

Local moment model and phase diagram.—In order to focus on the new physics induced by the RKKY interaction, we study a simplified Hamiltonian which retains the two key features described above, in the basis with a sublattice-dependent quantization axis along the local $\langle 111\rangle$ direction,

$$H = -\sum_{\boldsymbol{r},\boldsymbol{r}'} J_{\boldsymbol{r},\boldsymbol{r}'}[(1-w)\tau_s^z(\boldsymbol{r})\tau_{s'}^z(\boldsymbol{r}') + \boldsymbol{\tau}_s^{\perp}(\boldsymbol{r})\cdot\boldsymbol{\tau}_{s'}^{\perp}(\boldsymbol{r}')]. \quad (2)$$

Here, $J_{\boldsymbol{r},\boldsymbol{r}'} = J_1(J_2)$ for nearest (next-nearest) neighbor sites, $\tau_s^z(\boldsymbol{r})$ is the z component of the pseudospin on sublattice s at site $\boldsymbol{r}$, $\boldsymbol{\tau}_s^{\perp}(\boldsymbol{r})$ denotes the transverse component of the pseudospin which lies in the local XY plane, and w quantifies the exchange anisotropy. We set $J_1 = J\cos\theta$ and $J_2 = J\sin\theta$, and explore the phase diagram of this model as a function of (θ, w).

Treating the spins as classical unit vectors, we minimize the energy using a variational ansatz

$$\boldsymbol{\tau}_s(\boldsymbol{r}) = d_s\hat{\boldsymbol{e}}_3 + \sqrt{1-d_s^2}\,\text{Re}[(\hat{\boldsymbol{e}}_1 + i\hat{\boldsymbol{e}}_2)e^{i(\boldsymbol{Q}\cdot\boldsymbol{r}+\varphi_s)}], \quad (3)$$

with variational parameters d_s, $\hat{\boldsymbol{e}}_{1,2,3}$, $\boldsymbol{Q}$, φ_s where $\hat{e}_{1,2,3}$ form a triad of orthonormal vectors, so that $|\boldsymbol{\tau}_s(\boldsymbol{r})| = 1$, φ_s is a sublattice-dependent phase, and $|d_s| \leq 1$. In the local coordinate system, this ansatz allows, (i) for $d_s = 0$, a coplanar spiral with wave vector $\boldsymbol{Q}$ with spins in the $(\hat{e}_1, \hat{e}_2)$ plane, and, (ii) for $d_s^2 = 1$, a collinear state with spins along $\pm\hat{e}_3$. In the isotropic limit, $w = 0$, this ansatz recovers $(0, 0, q)$ spirals [28], while in the Ising limit it allows for two-in-two-out or all-in-all-out states. The complete ground state phase diagram from this variational analysis is shown in Fig. 1.

For $w > 0$, we find states where the spins lie in the local XY plane, forming phases like ferromagnetic XY, antiferromagnetic XY, or degenerate XY versions of two-in-two-out states. With increasing θ, the different shades (colors) in the AF-XY region represent states with distinct ordering wave vectors $\boldsymbol{Q} = (0q\pi), (0, 0, 0), (00q)$.

For $w < 0$, by contrast, we find, in addition to well known states like the ferromagnetic Ising (all-in-all-out), and Ising spin ice (two-in-two-out), large parameter regimes which support coexistence phases (CE_1, CE_2) with coplanar order involving spatially modulated Ising (magnetic dipolar) and XY (quadrupolar) order. The CE_1 and CE_2 states order at the wave vectors $(0, q, \pi)$ and $(0, 0, q)$, respectively, (or their symmetry related

momenta). Such CE states are "magnetoquadrupolar" supersolids which break time-reversal symmetry (defined by $\tau^z \to -\tau^z$), and most lattice symmetries. Below, we focus on the remarkable physical properties including the AHE of the CE_2 state which is (i) robustly present in an unbiased numerical energy minimization using a simulated annealing approach [29], and (ii) stable to the addition of weak perturbations such as $\tau^{\pm}\tau^{\pm}$ or second neighbor Dzyaloshinskii-Moriya interactions to the simple Hamiltonian in Eq. (2).

AHE and magnetization in the CE_2 *state.*—When the A site is in the CE_2 state, it imprints effective spatially varying magnetic fields and chemical potentials on the B-site conduction electrons due to the Kondo-type coupling. For an ordering wave vector $\boldsymbol{Q}$, this mixes electrons with wave vectors $\boldsymbol{k}$ and $\boldsymbol{k}+\boldsymbol{Q}$, leading to a Hamiltonian,

$$H^B_{\rm tb}(\boldsymbol{k}) = \begin{pmatrix} c^\dagger_{\boldsymbol{k},s,\sigma} & c^\dagger_{\boldsymbol{k}+\boldsymbol{Q},s,\sigma}\end{pmatrix}\tilde{H}_{\boldsymbol{k},\boldsymbol{Q}}\begin{pmatrix} c_{\boldsymbol{k},s,\sigma} \\ c_{\boldsymbol{k}+\boldsymbol{Q},s,\sigma}\end{pmatrix}$$
$$\tilde{H}_{\boldsymbol{k},\boldsymbol{Q}} = \begin{pmatrix} H_{\rm tb}(\boldsymbol{k}) & H_{AB}(\boldsymbol{Q}) \\ H_{AB}(-\boldsymbol{Q}) & H_{\rm tb}(\boldsymbol{k}+\boldsymbol{Q})\end{pmatrix}. \quad (4)$$

Here, s is the sublattice (0, 1, 2, 3) and σ is the pseudospin ($\uparrow, \downarrow$) index. $\tilde{H}_{\boldsymbol{k},\boldsymbol{Q}}$ is composed of 8×8 matrices: $H_{\rm tb}(\boldsymbol{k})$ is the Hamiltonian matrix of Eq. (1) at wave vector $\boldsymbol{k}$; $H_{AB}(\boldsymbol{Q})$ is the Hamiltonian matrix of $H_{AB}(c_1, c_2, c_3)$ given in the Supplemental Material [27]. For the CE_2 state in our anisotropic J_1-J_2 pseudospin model, $\boldsymbol{Q} = (00q)$, and time-reversal symmetry and all lattice symmetries except C_{2z} (π rotation along $\hat{z}$ direction) are broken; this leads to an intrinsic AHE. While the C_{2z} symmetry forces $\sigma_{yz} = \sigma_{xz} = 0$, since the current operator $\mathcal{J}_z$ is invariant under C_{2z} rotation $(x, y, z) \to (-x, -y, z)$ but the currents $\mathcal{J}_y$ and $\mathcal{J}_x$ change sign, σ_{xy} remains unchanged under this rotation and can, thus, be nonzero.

We consider the A site incommensurate CE_2 local moment order with wave vector $\boldsymbol{Q} \approx 1.2\pi(001)$, which is appropriate for $\theta = 1.72\pi$, $w = -0.5$ in Eq. (2) ($\star$ marked in Fig. 1), and the Kondo coupling constant $c/t = 0.1$ where $c_1 = 0$, $c_2 = c_3 = c$ in $H_{AB}(\boldsymbol{Q})$. (See the Supplemental Material [27].) Figure 2 shows an example of the reconstructed B-site band structure based on Eq. (4) [the horizontal (red) line indicates the Fermi level], with a choice of $t = 1$, $t' = -0.1$, and $|\boldsymbol{v}_{ij}| = 0.2$ in Eq. (1), which are close to those determined from the Slater-Koster parameters [26]. The reconstructed band structure contains, both, Weyl points and Fermi pockets near Γ, $\Gamma + \boldsymbol{Q}$. There are four pairs of Weyl points in total (two pairs near Γ, $\Gamma + \boldsymbol{Q}$ and the other two pairs at their C_{2z} symmetry related points) and the inset of Fig. 2 shows one of those Weyl points and Fermi pockets near $\boldsymbol{k} \approx (0, 0.12\pi, 0.02\pi)$. The B-site band reconstruction is weak, and we have checked that slight deviations from the quadratic band touching of the Ir band structure, such as having a small gap or small Fermi pockets (gap and pocket size less than one tenth of the total bandwidth), do not significantly modify the short-distance RKKY interactions; this obviates the need to consider the feedback of the reconstructed band dispersion on the RKKY interactions.

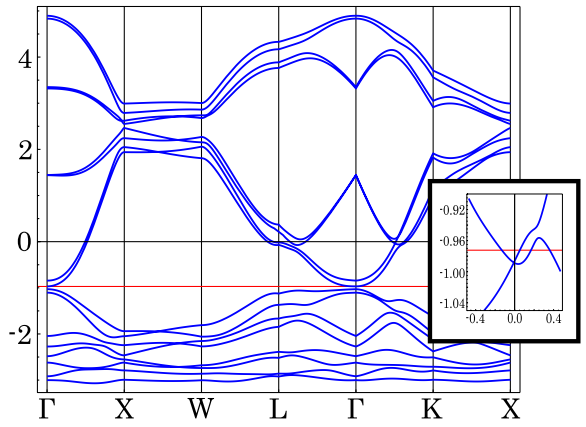

FIG. 2 (color online). Reconstructed $5d$ conduction electron band structure (based on Eq. (4) with the energy units of t) in the presence of Kondo coupling constant $c/t = 0.1$ and the A site incommensurate CE_2 local moment order with wave vector $\boldsymbol{Q} \approx 1.2\pi(001)$. The inset shows one Weyl point and Fermi pockets near $\boldsymbol{k} \approx (0, 0.12\pi, 0.02\pi)$ [the horizontal axis represents k along $\boldsymbol{k} = (k, k + 0.12\pi, 0.02\pi)$]. Its pair is located at $\boldsymbol{k} \approx (0.06\pi, 0.18\pi, 0)$.

Figure 3 shows the explicitly calculated AHE using the Kubo formula, as a function of Kondo coupling constant c, for the reconstructed B-site bands (see the Supplemental Material [27]). The strength of Kondo coupling c determines the magnitude of the AHE response. σ_{xy} initially increases with increasing c, acquiring contributions from small electronlike and holelike Fermi pockets as well as four pairs of Weyl points induced by the CE_2 order. For $c/t \gtrsim 0.7$, a band gap opens up and $\sigma_{xy} = 0$.

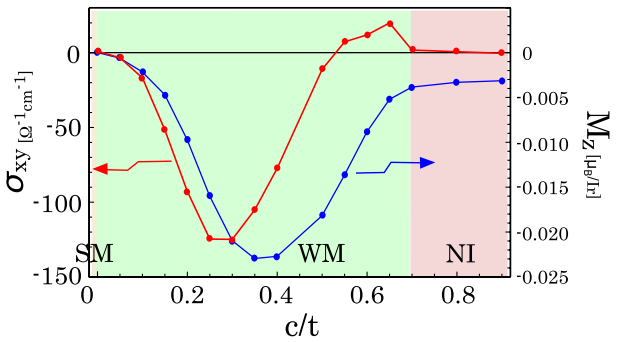

FIG. 3 (color online). Hall conductivity σ_{xy} and magnetization M_z as a function of the Kondo coupling constant c based on the reconstructed band structure (shown in Fig. 2 for $c/t = 0.1$). For $c = 0$, the conduction band is in a semimetal phase (SM) with a quadratic band touching at the Γ point. For $0 < c/t \lesssim 0.7$, the CE_2 state reconstructs the bands generating both Fermi pockets and pairs of Weyl points, resulting in a Weyl-metallic phase (WM). For $c/t \gtrsim 0.7$, the conduction electrons form a gapped normal insulating phase (NI).

On symmetry grounds, the AHE must be accompanied by a nonzero uniform magnetization, with $M_x = M_y = 0$ but $M_z \neq 0$. Remarkably, although the CE_2 state has no net magnetization from the local moments, we find that it induces a nonzero magnetization M_z for the $5d$ electrons, where $M_\mu = (1/N)\langle \sum_i \sum_{\alpha\beta} c^\dagger_{i\alpha}(\sigma^\mu_{\alpha\beta}/2)c_{i\beta}\rangle \equiv (1/N)\sum_i \langle j^\mu_i\rangle$. For small c, the net magnetization M_z gets larger, proportional to the density of states near the Fermi level, with the same sign and a trend qualitatively similar to σ_{xy}. For large $c/t \gtrsim 0.7$, we find that $M_z \neq 0$ although $\sigma_{xy} = 0$, signalling a magnetized band insulator.

This dichotomy of a large σ_{xy} but a small M can be argued for as follows. On dimensional grounds, the AHE signal $\sigma_{xy} \sim (e^2/h)\Delta k$, where the momentum scale Δk must be induced by an effective "internal magnetic field" $B^{\rm int}$ due to the spontaneous breaking of time-reversal symmetry [9,30]. If the $\tau^{x,y}$ order in the CE_2 state reconstructs the band structure to produce a small Fermi pocket, with a Fermi wave vector k_F and an effective mass m^*, we expect $k_F \Delta k/m^* \sim B^{\rm int}$ resulting in a large σ_{xy} due to a small k_F Fermi pocket, while the magnetization $M \sim B^{\rm int} m^* k_F$ stays small. The Weyl point contribution from splitting a quadratic band touching, with a curvature m^{**}, on the other hand leads to $\Delta k \sim \sqrt{m^{**} B^{\rm int}}$ [31], and a magnetization $M \sim B^{\rm int}$, so that a small $B^{\rm int}$ again leads to a large σ_{xy} and a small M. The presence of both contributions leads to a nonlinear $\sigma_{xy}(M_z)$ (see the Supplemental Material [27]).

Application to $Pr_2Ir_2O_7$.—The CE_2 state in our simple model of RKKY coupled non-Kramers ions and spin-orbit coupled conduction electrons captures a key aspect of experiments on $Pr_2Ir_2O_7$: an AHE accompanied by a negligible magnetization. However, since our ordering wave vector is along the $\langle 001\rangle$ direction, the spontaneous AHE is produced in the XY plane, whereas the spontaneous AHE in $Pr_2Ir_2O_7$ is seen for fields along the $\langle 111\rangle$ direction. This discrepancy may be resolved if the spiral order had a wave vector along the $\langle 111\rangle$ direction, or if our CE order gave way to a multimode spiral formed by superposing $(0, 0, q)$, $(0, q, 0)$, $(q, 0, 0)$ spirals while preserving C_3 rotation along the $\langle 111\rangle$ direction but breaking all other lattice symmetries. The Hall conductivity will then be in the plane perpendicular to $\langle 111\rangle$, in agreement with experiment. Based on our Kubo calculation, we estimate the magnitude of the AHE (at $c/t = 0.1$, which is $c \approx 5$ meV) in our CE_2 state to be $\sigma_{xy} \approx -15(\Omega^{-1}\,{\rm cm}^{-1})$ and $M_z \approx -0.002(\mu_B/{\rm Ir})$. This is consistent with the magnitude of the measured Hall signal $\sim -5\ \Omega^{-1}\,{\rm cm}^{-1}$, with an unmeasurably small $M_z \ll 0.01\mu_B$.

The Curie-Weiss temperature is sensitive to J_2/J_1, changing sign as a function of θ even within the CE_2 state. For couplings $c/t \sim 0.1$, we can obtain $\theta_{\rm CW}$ to be of the right sign and magnitude, $\theta_{\rm CW} \sim -20$ K as observed experimentally, for parameter values closer to the all-in-all-out phase boundary.

The CE_2 state should exhibit two distinct thermal transitions, associated with the onset of Ising and XY orders, with the splitting between them being smaller for a weaker anisotropy w, as we confirm using Monte Carlo simulations [32]. This simple expectation may get confounded by two issues. (i) Terms which we have omitted, $\propto \tau^\pm_i \tau^\pm_j$, will break the (staggered) U(1) invariance of the XY terms, and modify the 3d-XY universality class of the quadrupolar ordering transition. (ii) Oxygen vacancy defects will break the D_{3d} point group symmetry around the Pr^{3+} ion, splitting the non-Kramers doublet due to extra random terms $\Delta H_{\rm cef} \propto \{J_z, J_\pm\} \sim \tau^\pm$ in the effective crystal field Hamiltonian, leading to a time-reversal invariant strong random field on $\tau^{x,y}$. These effects might conspire to smear or destroy the XY ordering transition. However, the time-reversal symmetry breaking Ising transition is expected to survive, which would be consistent with the single specific heat "peak" seen at the onset of the AHE in $Pr_2Ir_2O_7$. We note that the observed spontaneous AHE necessarily implies at least one thermal phase transition associated with spontaneously broken time-reversal symmetry.

The most direct evidence for our scenario would be a detection of the modulated Ising order using neutron diffraction. Landau theory arguments predict that such a coexistence phase should support a weak charge density wave of the Ir electrons at the ordering wave vector of the spiral, from a term $\propto \tau^{x,y}(\boldsymbol{q})n(-\boldsymbol{q})$, which we find small but finite in our calculations; this can be probed, in principle, using x-ray diffraction. In the presence of an induced charge order, Landau theory predicts a nonzero d-band magnetization, from a term $\propto M\tau^z(\boldsymbol{q})n(-\boldsymbol{q})$, which is indeed present as discussed above.

Conclusion.—We have proposed a mechanism of intrinsic AHE in metallic pyrochlore systems, such as $Pr_2Ir_2O_7$, arising from spiral order of local moments driven by their extended anisotropic RKKY exchange interactions, and the resulting reconstruction of the electronic band structure to form small Fermi pockets and pairs of Weyl points. This ordering could occur proximate to an all-in-all-out state of the local moments, and appears to be distinct from previously proposed spin-chirality scenarios [16,19–21] for the AHE in $Pr_2Ir_2O_7$.

We are grateful to Subhro Bhattacharjee, Hae-Young Kee, Eric Kin-Ho Lee, and Jeffrey Rau for useful discussions. This work was supported by NSERC, CIFAR, and the Center for Quantum Materials at the University of Toronto.

[1] L. Savary and L. Balents, Phys. Rev. Lett. **108**, 037202 (2012).
[2] S. B. Lee, S. Onoda, and L. Balents, Phys. Rev. B **86**, 104412 (2012).
[3] D. Pesin and L. Balents, Nat. Phys. **6**, 376 (2010).
[4] B.-J. Yang and Y. B. Kim, Phys. Rev. B **82**, 085111 (2010).

[5] X. Wan, A. M. Turner, A. Vishwanath, and S. Y. Savrasov, Phys. Rev. B **83**, 205101 (2011).
[6] W. Witczak-Krempa and Y. B. Kim, Phys. Rev. B **85**, 045124 (2012).
[7] A. Go, W. Witczak-Krempa, G. S. Jeon, K. Park, and Y. B. Kim, Phys. Rev. Lett. **109**, 066401 (2012).
[8] X. Wan, A. Vishwanath, and S. Y. Savrasov, Phys. Rev. Lett. **108**, 146601 (2012).
[9] A. A. Burkov and L. Balents, Phys. Rev. Lett. **107**, 127205 (2011).
[10] D. Yanagishima and Y. Maeno, J. Phys. Soc. Jpn. **70**, 2880 (2001).
[11] K. Matsuhira, Makoto Wakeshima, R. Nakanishi, T. Yamada, A. Nakamura, W. Kawano, S. Takagi, and Y. Hinatsu, J. Phys. Soc. Jpn. **76**, 043706 (2007).
[12] K. Matsuhira, Y. Hinatsu, K. Tenya, H. Amitsuka, and T. Sakakibara, J. Phys. Soc. Jpn. **71**, 1576 (2002).
[13] S. Bramwell, M. Field, M. Harris, and I. Parkin, J. Phys. Condens. Matter **12**, 483 (2000).
[14] S. Nakatsuji, Y. Machida, Y. Maeno, T. Tayama, T. Sakakibara, J. Duijn, L. Balicas, J. Millican, R. Macaluso, and Julia Chan, Phys. Rev. Lett. **96**, 087204 (2006).
[15] Y. Machida, S. Nakatsuji, Y. Maeno, T. Tayama, T. Sakakibara, and S. Onoda, Phys. Rev. Lett. **98**, 057203 (2007).
[16] Y. Machida, S. Nakatsuji, S. Onoda, T. Tayama, and T. Sakakibara, Nature (London) **463**, 210 (2009).
[17] Y. Taguchi, Y. Oohara, H. Yoshizawa, N. Nagaosa, Y. Tokura, Science **291**, 2573 (2001).
[18] N. Nagaosa, J. Sinova, S. Onoda, A. H. MacDonald, and N. P. Ong, Rev. Mod. Phys. **82**, 1539 (2010).
[19] A. Kalitsov, B. Canals, and C. Lacroix, J. Phys. Conf. Ser. **145**, 012020 (2009).
[20] M. Udagawa and R. Moessner, Phys. Rev. Lett. **111**, 036602 (2013).
[21] R. Flint and T. Senthil, Phys. Rev. B **87**, 125147 (2013).
[22] J. Ye, Y. Kim, A. Millis, B. Shraiman, P. Majumdar, and Z. Tešanović, Phys. Rev. Lett. **83**, 3737 (1999).
[23] G. Chen and M. Hermele, Phys. Rev. B **86**, 235129 (2012).
[24] The presence of Fermi pockets does not allow us to separate the band and Weyl point contributions to σ_{xy}.
[25] S. Onoda and Y. Tanaka, Phys. Rev. Lett. **105**, 047201 (2010).
[26] E. K.-H. Lee, S. Bhattacharjee, and Y. B. Kim, Phys. Rev. B **85**, 224428 (2012).
[27] See Supplemental Material at http://link.aps.org/supplemental/10.1103/PhysRevLett.111.196601 for the local coordinate information of *A*-site pyrochlore lattice, the explicit forms of the Kondo coupling and the RKKY interaction, pseudospin configuration of spiral coexistence state, and the nonlinear behavior of the Hall coefficient as a function of net magnetization.
[28] M. F. Lapa and C. L. Henley, arXiv:1210.6810.
[29] We find that the variational ansatz captures most of the phases found in the simulated annealing approach. Our ansatz does not capture regimes where multiple-$\boldsymbol{Q}$ orders are favored—such states are well known to occur in the isotropic case $w = 0$ where we find the CE_1 order, and will be discussed in a future work.
[30] K.-Y. Yang, Y.-M. Lu, and Y. Ran, Phys. Rev. B **84**, 075129 (2011).
[31] E.-G. Moon, C. Xu, Y. B. Kim, and L. Balents, arXiv:1212.1168.
[32] S. B. Lee *et al.* (unpublished).